Second-harmonic generation from split-ring resonators on a GaAs substrate

F. B. P. Niesler,[1,*] N. Feth,[1,2] S. Linden,[1,2,3] J. Niegemann,[3,4] J. Gieseler,[4] K. Busch,[3,4] and M. Wegener[1,2,3]

[1]*Institut für Angewandte Physik, Universität Karlsruhe (TH), D-76128 Karlsruhe, Germany*
[2]*Institut für Nanotechnologie, Forschungszentrum Karlsruhe in der Helmholtz-Gemeinschaft, D-76021 Karlsruhe, Germany*
[3]*DFG–Center for Functional Nanostructures, Universität Karlsruhe (TH), D-76128 Karlsruhe, Germany*
[4]*Institut für Theoretische Festkörperphysik, Universität Karlsruhe (TH), D-76128 Karlsruhe, Germany*
**Corresponding author: fabian.niesler@physik.uni-karlsruhe.de*

Received March 27, 2009; revised April 29, 2009; accepted May 4, 2009;
posted May 14, 2009 (Doc. ID 109365); published June 25, 2009

We study second-harmonic generation from gold split-ring resonators on a crystalline GaAs substrate. By systematically varying the relative orientation of the split-ring resonators with respect to the incident linear polarization of light and the GaAs crystallographic axes, we unambiguously identify a nonlinear contribution that originates specifically from the interplay of the local fields of the split-ring resonators and the bulk GaAs second-order nonlinear-susceptibility tensor. The experimental results are in good agreement with theoretical modeling. © 2009 Optical Society of America

OCIS codes: 000.4430, 160.4330, 190.3970.

Recent research on photonic metamaterials, composed of densely packed split-ring resonators (SRRs) and variations thereof, has largely focused on magnetic responses and negative refractive indices [1–3]. Yet obtaining an enhanced nonlinear optical response from metamaterials is another interesting avenue that was already suggested in the original publication on the SRR [1]. The authors envisioned adding a nonlinear material in the gap of the SRR that can be viewed as the capacitive part of a miniature resonant *LC* circuit. Further theoretical work followed the same spirit [4]. Recent experimental work [5–8], however, rather explored the intrinsic nonlinearity of the metal nanostructure itself, because the glass substrate used there did not have a significant nonlinear optical response. Other experimental work has addressed plasmonic nanostructures on a GaAs substrate [9], actual nonlinear spectroscopy [10] on photonic metamaterials, and the role of higher-order moments [11]. Notably, recent experiments on arrays of plasmonic bow-tie antennae interacting with noble gases have even shown enhanced high-harmonic generation [12] up to the 17th order–providing further motivation that the nonlinear optics of photonic metamaterials is indeed a very promising avenue.

In this Letter, we experimentally and theoretically investigate second-harmonic generation (SHG) from arrays of SRRs on a (noncentrosymmetric) crystalline GaAs substrate, aiming at coming closer to the original theoretical suggestion [1] and at possibly achieving more-efficient frequency conversion than for SRRs on glass. For the latter, we have previously estimated [6,7] the conversion efficiency to be comparable with a similarly thick piece of potassium dideuterium phosphate with $\chi^{(2)}=1.0\times10^{-12}$ m/V.

The SRR samples employed in our work are fabricated by standard electron-beam lithography and high-vacuum electron-beam deposition of 25 nm gold onto commercially available crystalline GaAs substrates of several hundreds of micrometers in thickness—essentially a half-space geometry. We have found that the SHG signal from gold SRRs directly on GaAs deteriorates with time under the influence of intense optical excitation. We tentatively ascribe this undesired effect (which had not occurred at all previously for glass substrates [5–8]) to light-induced diffusion of the metal into the semiconductor. To eliminate this artifact, we deposit a 10 nm thin film of MgF_2 onto the GaAs as a diffusion barrier. With this measure and at the light levels used below, the SHG signals turn out to be stable over many days. The footprint of all samples discussed here is 60 μm × 60 μm. Figure 1 shows a selected electron micrograph of SRR from such an array as well as a corresponding measured normal-incidence reflectance spectrum for the relevant horizontal incident polarization. To get to about 1.5 μm fundamental resonance wavelength, these SRRs on the high-

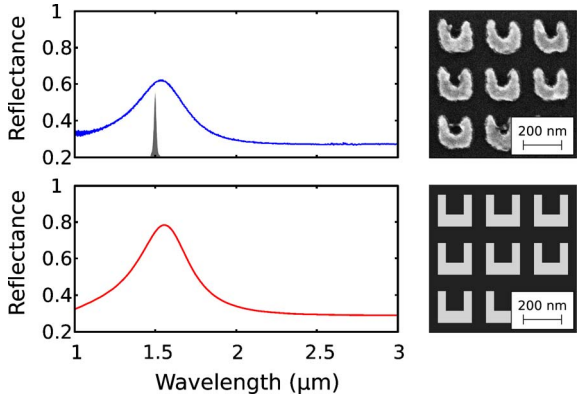

Fig. 1. (Color online) Top, example of a measured normal-incidence reflectance spectrum (taken from the air side) of lithographically defined SRR on a crystalline GaAs substrate. Incident linear polarization is horizontal. The narrow gray area illustrates the exciting laser spectrum centered at 1.5 μm wavelength. The sample corresponds to that in Fig. 3(b); the electron micrograph on the right-hand side shows selected SRR from this sample. Bottom, same but theory.

index GaAs substrate have to be about 30% smaller than their counterparts on glass substrate [5–8].

The exciting 170 fs Gaussian linearly polarized laser pulses obtained from an optical parametric oscillator (Spectra-Physics OPAL) operating at 86 MHz repetition frequency are tuned to this wavelength of 1.5 μm. 45 mW of average power is focused to a Gaussian spot of 60 μm in diameter. As SHG at 750 nm wavelength would clearly be absorbed by the GaAs substrate, we let the fundamental pulses impinge under normal incidence from the GaAs substrate side such that the SHG is emitted into air. This SHG signal is collected and spectrally dispersed by a grating spectrometer connected to a liquid-nitrogen-cooled silicon CCD camera. The count rates quoted below refer to the spectrally integrated signals. Owing to the finite quantum efficiency of the camera and to losses in the setup, the number of photons per second is approximately three times larger than the quoted count rates. For example, a count rate of 8×10^6/s corresponds to 2.4×10^7 SHG photons per second emitted by the sample. An analyzer in front of the spectrometer allows for analyzing the polarization state of the SHG radiation emitted into the forward direction by means of acquiring polar diagrams.

It is well known that (100) and (110) GaAs wafers are not equivalent regarding SHG under normal-incidence excitation [13]. Furthermore, the SRR can be oriented differently with respect to the GaAs crystallographic axes (illustrated in Fig. 2), and they can be excited by two orthogonal incident linear polarizations. Three different cases are depicted in Fig. 3, the most striking of which is (b). Here, by symmetry, for horizontal incident polarization of light (x direction, see also the unlettered arrow), SHG from the bare GaAs substrate is forbidden. Indeed, we find a SHG signal that is about 50 times weaker for the bare GaAs substrate (not shown) than from the SRR on GaAs. The emerging SHG polarization is almost horizontal (x direction). By symmetry, consistent with our previous experiments [5–8], SHG from the SRR alone can be polarized only vertically (y direction). *We can conclude that the measured horizontal component of the SHG signal in Fig. 3(b) stems specifically from the interplay of crystalline GaAs substrate and the SRR.* An additional vertically polarized contribution from the bare SRR [5–8] could explain the slight (20 deg)

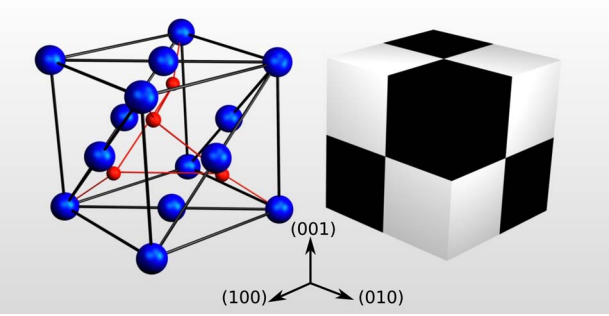

Fig. 2. (Color online) (left) GaAs zinc-blende crystal structure and (right) schematic representation by a "checkerboard cube" (used in Fig. 3).

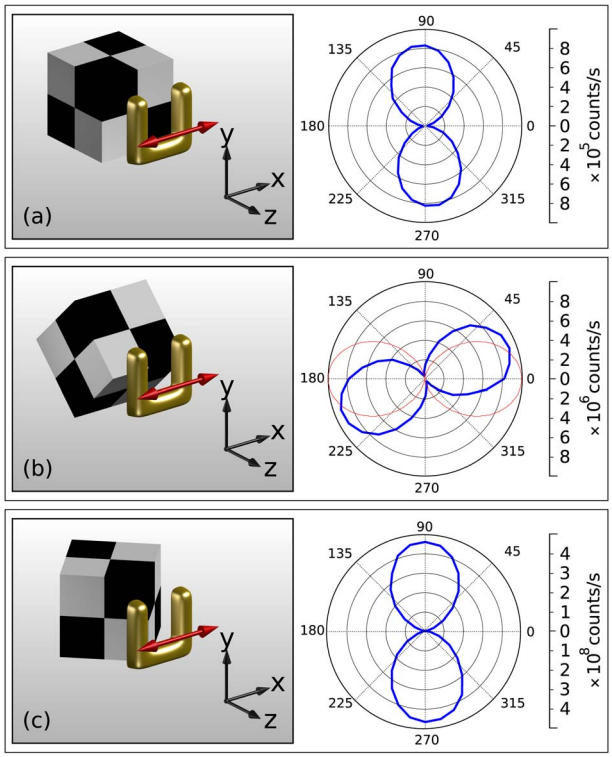

Fig. 3. (Color online) (a)–(c) SHG from three different samples: (a) (100) GaAs; (b) and (c) (110) GaAs. The orientation of the GaAs crystal (compare Fig. 2), SRR, and the incident horizontal linear polarization (unlettered arrow) is illustrated in the left column. Light impinges under normal incidence ($+z$ direction). SHG is detected into the forward direction (also $+z$). The right column shows measured polar diagrams (dark, blue curves) of the emerging SHG signal, where the horizontal (vertical) axis with respect to the panel plane is the x (y) direction. The experiment in (b) can be directly compared with theory (light, red curve).

rotation of the figure eight in Fig. 3(b). The SHG signals from the SRR on GaAs are a factor of 25 larger than those previously observed by us from the SRR on the glass substrate [5–8] (when scaled to the same incident power level).

The SHG signal in Fig. 3(a) is about 1 order of magnitude smaller than in Fig. 3(b). Excitation of the bare GaAs under the conditions of Fig. 3(a) leads to a signal that is about 40 times weaker (not shown). This is consistent with the fact that SHG from the bare GaAs is not allowed under the condition of Fig. 3(a). However, in this case, the vertically polarized SHG signal could, by symmetry, stem from the bare SRR. The situation is reversed in Fig. 3(c) in that, here, SHG from the bare GaAs substrate is allowed. As a result, the signal levels are much higher than for both (a) and (b), because the SHG signal in (c) originates mainly from the GaAs crystal [13] (albeit badly phase mismatched), whereas (b) stems mainly from the SRR evanescent near field in the GaAs crystal.

To further strengthen our above assignment of the SHG mechanism for (110) GaAs and horizontal incident polarization in Fig. 3(b), we inspect the bulk $\chi^{(2)}$ susceptibility tensor. In the $x-y-z$ coordinate system of Fig. 3 we get the nonvanishing transverse ($x-y$)

second-order bulk contributions to the macroscopic optical SHG polarization from [13]

$$P_x^{(2)} = \epsilon_0 \chi^{(2)}_{x,z,z} E_z E_z - \epsilon_0 \chi^{(2)}_{x,y,y} E_y E_y, \quad (1)$$

$$P_y^{(2)} = -\epsilon_0 \chi^{(2)}_{y,x,y} E_x E_y - \epsilon_0 \chi^{(2)}_{y,y,x} E_y E_x, \quad (2)$$

with $\chi^{(2)}_{x,z,z} = \chi^{(2)}_{x,y,y} = \chi^{(2)}_{y,x,y} = \chi^{(2)}_{y,y,x}$. A snapshot of the components of the electric-field vector (E_x, E_y, E_z) at the peak of the 170 fs Gaussian pulse centered around 1.5 μm wavelength inside the GaAs substrate just below the 10 nm thin MgF_2 spacer layer is depicted in Fig. 4. These fields are obtained using a home-built finite-difference time-domain (FDTD) computer program solving the linear Maxwell equations for the experimental geometry (Fig. 1, bottom). The gold is described by the linear free-electron Drude model with plasma frequency $\omega_{\mathrm{pl}} = 2\pi \times 2.2 \times 10^{15}\ \mathrm{s}^{-1}$ and collision frequency $\omega_{\mathrm{coll}} = 2\pi \times 1.72 \times 10^{13}\ \mathrm{s}^{-1}$. The linear GaAs refractive index is taken as $n_{\mathrm{GaAs}} = 3.37$ and that of the MgF_2 layer as $n_{\mathrm{MgF_2}} = 1.34$. The resulting reflectance spectrum is shown in Fig. 1.

Within the spirit of an effective medium, the effective transverse SHG polarization is the spatial average over one unit cell, with components $\langle P_x^{(2)} \rangle$ and $\langle P_y^{(2)} \rangle$. From Fig. 4 it becomes immediately clear that $\langle P_y^{(2)} \rangle \propto \langle E_x E_y \rangle = 0$, whereas $\langle P_x^{(2)} \rangle \propto \langle (E_z E_z - E_y E_y) \rangle \neq 0$. Thus, the emerging SHG is expected to be horizontally polarized [see light curve in Fig. 3(b)]. It can also be seen from Fig. 4 that this SHG signal is driven mainly by the overwhelming axial component $E_z E_z$. In contrast, without any SRRs, the incident E_x component alone cannot generate SHG at all, consistent with our experimental observations and with literature. As nonlinearities from the metal are not accounted for at this point, our treatment also delivers strictly zero SHG signal for the bare SRR. Thus, under the conditions of Fig. 3(b), the calculated SHG signal arises specifically from the *combined* system of the SRR and GaAs. Either alone gives no SHG at all. This overall reasoning is further supported by more complete FDTD solutions of the nonlinear Maxwell equations, the details of which shall be published elsewhere.

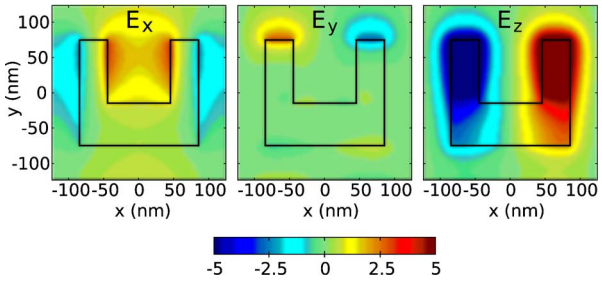

Fig. 4. (Color online) Snapshot of the local electric-field components underneath the SRR inside the GaAs for excitation at 1.5 μm wavelength. All components are equally normalized to the incident electric-field amplitude in the GaAs. One unit cell of the SRR array is shown; the geometry corresponds to Fig. 3(b).

In conclusion, we have observed SHG from SRR arrays on a crystalline GaAs substrate. Referenced to the same incident laser intensity, these SHG signals are 25 times larger than those from SRR on glass substrate.

The project PHOME acknowledges financial support by the European Commission, the project METAMAT by the Bundesministerium für Bildung und Forschung.

References

1. J. B. Pendry, A. J. Holden, D. J. Robbins, and W. J. Stewart, IEEE Trans. Microwave Theory Tech. **47**, 2075 (1999).
2. V. M. Shalaev, Nat. Photonics **1**, 41 (2007).
3. C. M. Soukoulis, S. Linden, and M. Wegener, Science **315**, 47 (2007).
4. A. A. Zharov, I. V. Shadrivov, and Y. S. Kivshar, Phys. Rev. Lett. **91**, 037401 (2003).
5. M. W. Klein, C. Enkrich, M. Wegener, and S. Linden, Science **313**, 502 (2006).
6. M. W. Klein, M. Wegener, N. Feth, and S. Linden, Opt. Express **15**, 5238 (2007).
7. M. W. Klein, M. Wegener, N. Feth, and S. Linden, Opt. Express **16**, 8055 (2008).
8. N. Feth, S. Linden, M. W. Klein, M. Decker, F. B. P. Niesler, Y. Zeng, W. Hoyer, J. Liu, S. W. Koch, J. V. Moloney, and M. Wegener, Opt. Lett. **33**, 1975 (2008).
9. W. Fan, S. Zhang, K. J. Molloy, S. R. J. Brueck, N. C. Panoiu, and R. M. Osgood, Opt. Express **14**, 9570 (2006).
10. E. Kim, F. Wang, W. Wu, Z. Yu, and Y. R. Shen, Phys. Rev. B **78**, 113102 (2008).
11. S. Kujala, B. K. Canfield, M. Kauranen, Y. Svirko, and J. Turunen, Opt. Express **16**, 17196 (2008).
12. S. Kim, J. Jin, Y. J. Kim, I. Y. Park, Y. Kim, and S. W. Kim, Nature **453**, 757 (2008).
13. R. W. Boyd, *Nonlinear Optics* (Academic, 2003).